Crystallization and Melting Behavior of Poly(3-butylthiophene), Poly(3-octylthiophene), and Poly(3-dodecylthiophene)

Valerio Causin,* Carla Marega, and Antonio Marigo

Dipartimento di Scienze Chimiche, Università di Padova, via Marzolo 1, 35131 Padova, Italy

Luca Valentini and Josè Maria Kenny

Dipartimento di Ingegneria Civile e Ambientale, Università di Perugia, Loc. Pentima Bassa 21, 05100 Terni, Italy

Received September 8, 2004; Revised Manuscript Received November 2, 2004

ABSTRACT: The crystallization and melting behavior of poly(3-butylthiophene) (P3BT), poly(3-octylthiophene) (P3OT), and poly(3-dodecylthiophene) (P3DDT) were studied. The equilibrium melting temperatures (T_m^0) of these polymers were measured and resulted equal to 321, 230, and 175 °C for P3BT, P3OT, and P3DDT, respectively. The crystallization kinetics was evaluated by the Avrami equation: it proceeds by heterogeneous nucleation with one-dimensional linear growth ($n = 1.1-1.8$). The effects of the length of the alkyl side chain and of the undercooling were investigated. Phase I, Phase II, and a nematic mesophase were detected in P3BT and P3DDT. In P3BT, Phase I was differentiable from the mesophase on the basis of wide-angle X-ray scattering (WAXS) patterns. This study gives insight, in particular, on the crystallization and melting behavior of P3BT, a polymer not yet well studied. WAXS, small-angle X-ray scattering (SAXS), and differential scanning calorimetry (DSC) were employed as experimental techniques.

Introduction

Poly(3-alkylthiophene)s (P3ATs) have attracted in the past few years much attention because the alkyl modification, while improving the solubility, fusibility, and processability of the polymers does not alter their stability and electrical conductivity.[1−5] These properties place these polymers among the most promising ones for technological applications such as light-emitting diodes, field-effect transistors, batteries, sensors, and electrochromic devices. The structure of P3ATs has been studied by several groups,[6−10] and agreement has been reached on the fact that these systems are semicrystalline. The crystalline fraction consists of stacked layers constructed of a side-by-side arrangement of comblike polymer chains.[8] The flexible alkyl side chains function as spacers between the stiffer polythiophene main chains, the separation distance depending on the alkyl side chain length. Moreover, a polymorphic behavior for these systems has been reported.[11−16] Phase II, with respect to the more common Phase I, is characterized by a shorter distance associated with the first strong Bragg diffraction maximum in X-ray diffraction spectra. It has been suggested[14] that in Phase II interdigitation, in which the side chains are intercalated, is prevalent. On the other hand, in Phase I interdigitation is minimal,[14] and an end-to-end arrangement is typical of this polymorph.[6] The appearance of a nematic mesophase has also been reported.[6,11−15,17,18] Furthermore, head-to-tail (H−T) regioregularity plays an important role in determining many properties of these polymers, such as crystallinity, conductivity, and conduction mechanisms.[19] The alkyl group can be, in fact, incorporated in the thiophene ring with two different regioregularities: head-to-head and head-to-tail, the latter being preferable since it improves electroconductivity, optical nonlinearity, and magnetic properties.[3] Thus far, crystallization of P3ATs has been covered by just a few papers: Park and Levon[20] and Liu and Chung[21] studied poly(3-dodecylthiophene) (P3DDT), while Malik and Nandi[19] focused on poly(3-hexylthiophene) (P3HT), poly(3-octylthiophene) (P3OT), and P3DDT. To the authors' knowledge, no such studies have been presented for poly(3-butylthiophene) (P3BT). In the present paper, the crystallization and melting behavior of P3BT, P3OT, and P3DDT will be investigated and compared. Evidence of the formation of Phase II in P3BT and P3DDT will be shown. Wide- and small-angle X-ray scattering (WAXS and SAXS, respectively) and differential scanning calorimetry (DSC) were employed as experimental techniques. The effect of alkyl substitution and undercooling, a parameter never considered before, on the structure of these polymers will be discussed.

Experimental Section

Samples. Regioregular P3BT, P3OT, and P3DDT were purchased from Aldrich Chemical Co. The samples were synthesized by the Rieke method.[3] H−T regioregularity was reported by the company to be >97% for P3BT and >98.5% for P3OT and P3DDT. The molecular weight was reported just for P3OT ($\bar{M}_w = 142\,000$ and $\bar{M}_n = 54\,000$) and for P3DDT ($\bar{M}_w = 162\,000$).

Sample Preparation. The samples used for diffractometric experiments were melted between two aluminum plates at 270, 200, and 170 °C (for P3BT, P3OT, and P3DDT, respectively) for 5 min and then rapidly transferred into an oven preset at the desired crystallization temperature (T_c). The crystallization time was selected to be long enough for the process to be completed and evaluated on the basis of DSC data. The thermostat of the oven had a drift range of ±0.4 °C, and it was accurately checked that opening the door while inserting the sample holder caused a lowering of the inner set temperature of less than 1 °C. Three series of samples were prepared having undercoolings of 60, 75, and 90 °C, respectively. Undercooling (ΔT) is given by the difference between T_m^0 and T_c: $\Delta T = T_m^0 - T_c$.

DSC measurements were performed on the polymers without any kind of preliminary processing.

* To whom correspondence should be addressed. Phone: +39-049-8275153. Fax: +39-049-8275161. E-mail: valerio.causin@unipd.it.

10.1021/ma048159+ CCC: $30.25
Published on Web 12/24/2004

Differential Scanning Calorimetry. All measurements were carried out with a TA Instruments model 2920 calorimeter operating under N_2 atmosphere. Polymer samples weighing about 5 mg closed in aluminum pans were used throughout the experiments. Indium of high purity was used for calibrating the DSC temperature and enthalpy scales.

Wide- and Small-Angle X-ray Scattering. The WAXS patterns were recorded in the diffraction angular range 2−50° 2θ by a Philips X'Pert PRO diffractometer. When gathering temperature-dependent WAXS spectra, an Anton Paar TTK450 temperature control cell was used and the angular range was limited to 2−35° 2θ.

The SAXS spectra of the samples were recorded by a MBraun system, utilizing the Cu Kα radiation from a Philips PW 1830 X-ray generator. The data were collected by a position-sensitive detector in the scattering angular range 0.1−5.0° 2θ, and they were successively corrected for the blank scattering.

Finally, the Lorentz correction was applied: $I_1(s) = 4\pi s^2 I(s)$, where $I_1(s)$ is the one-dimensional scattering function and $I(s)$ the desmeared intensity function, with $s = (2/\lambda)\sin\theta$.

Equilibrium Melting Temperature. T_m^0 of the samples was determined by the technique proposed by Hoffman and Weeks.[22] It was possible to obtain T_m^0 of the samples by plotting the peak melting temperatures (T_m) with respect to the crystallization temperatures (T_c). The crossing of the extrapolation of the melting temperatures and the line of unit slope $T_m = T_c$ gives T_m^0. The isothermal crystallizations were performed in the DSC by erasing the thermal history of the sample for 5 min at 270, 200, and 170 °C (for P3BT, P3OT, and P3DDT, respectively) and cooling at the maximum controllable rate to the desired crystallization temperature. After a suitable time the samples were heated again at 10 °C/min in order to obtain their melting temperatures.

Kinetics of Crystallization. The kinetics of crystallization was studied by subjecting each sample to the following thermal cycle: after erasing previous thermal history by keeping the polymer at 270, 200, and 170 °C (for P3BT, P3OT, and P3DDT, respectively) for 5 min, it was cooled at the maximum rate to the crystallization temperature (T_c). The heat evolved during the transition was monitored as a function of time during an isothermal at T_c of suitable length. The fraction X of material crystallized after time t was estimated from the relation

$$X = \left\{\int_0^t \left(\frac{dH}{dt}\right)dt\right\} / \left\{\int_0^\infty \left(\frac{dH}{dt}\right)dt\right\} \quad (1)$$

where the numerator is the heat generated at time t and the denominator is the total heat of crystallization. The Avrami equation[23−25] was used to correlate X with time

$$X = 1 - \exp[-K(t-\tau)^n] \quad (2)$$

K is the kinetic constant of crystallization and n is a coefficient linked to the time dependence and the dimensions of growth of crystallites. The induction time τ has been evaluated as the earliest point where the sample baseline is flat following the cooling from the melting temperature to the chosen T_c.

Results and Discussion

T_m^0 is the melting point of a perfect and infinitely large crystal. T_m^0 of the P3AT samples have been extrapolated by the Hoffman−Weeks procedure,[22] as shown in Figure 1.

It can be seen that the lines relative to the samples intersect the line of unit slope $T_m = T_c$ to yield T_m^0 of 321 ± 2, 230 ± 2, and 175 ± 2 °C for P3BT, P3OT, and P3DDT, respectively. The values for P3DDT and P3OT are in good agreement with those previously reported by Malik and Nandi,[19] while T_m^0 of P3BT was never measured before. An equilibrium melting point of 321 °C is in accord, though, with that expected on the basis of the extrapolation of T_m^0 vs the number of carbon atoms in the side chains, operated by the same authors.[19] Since it is known[26] that a high T_m^0 can be linked to intense and numerous intermolecular interactions in the crystalline state (e.g., polyamides that form extensive hydrogen bonding) or to the stiffness of chains in the liquid state (e.g., aromatic polyesters), our data suggest that the shorter the alkyl side chains are, the less flexible the whole polymer is.

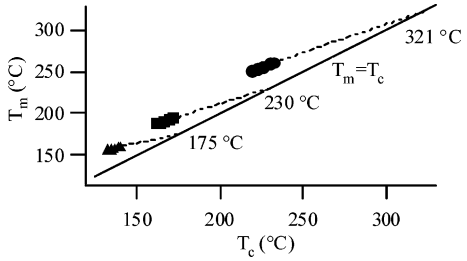

Figure 1. Hoffman−Weeks plot of P3BT (●), P3OT (■), and P3DDT (▲).

Table 1. Crystallization Kinetic Parameters n and K Obtained by the Avrami Analysis at the Temperatures T_c and Corresponding Undercooling ΔT for P3BT, P3OT, and P3DDT

T_c (°C)	ΔT (°C)	n	−ln K
	P3BT		
204	117	1.7	0.45
206	115	1.8	0.42
219	102	1.7	0.45
222	99	1.5	0.99
226	95	1.7	0.95
230	91	1.6	0.98
232	89	1.4	1.74
	P3OT		
160	70	1.2	1.96
162	68	1.2	1.79
164	66	1.2	1.97
166	64	1.2	2.01
168	62	1.3	2.04
170	60	1.2	1.98
172	58	1.3	2.11
	P3DDT		
133	42	1.2	2.14
135	40	1.3	2.28
137	38	1.3	2.33
139	36	1.3	2.34
141	34	1.3	2.36
162	13	1.1	2.22
164	11	1.3	2.00

This is confirmed by reported data on the work of chain folding, which increases with increasing length of side chain.[19] The crystallization kinetics, quantified by the Avrami equation, seems to support this hypothesis (Table 1). To attain comparable rate of crystallization constants K, it is necessary to impose much higher undercoolings for P3BT than P3DDT. The samples with longer alkyl side chains exhibit a faster rate because their molecules are more mobile and adaptable to fit into the crystalline framework.

Another piece of information that can be extracted from the data in Table 1 is the Avrami coefficient n. The measured n values are always comprised in the range 1.1−1.8. According to theory,[23−25] this means that crystallization of the examined P3ATs occurs by heterogeneous nucleation with one-dimensional linear growth. While for P3OT and P3DDT our data are in accord with the literature,[19] no such term of confrontation is available for P3BT. It appears though that n is quite independent of the length of the alkyl side chains.

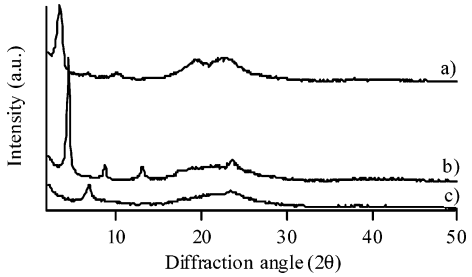

Figure 2. WAXS patterns of P3DDT (a), P3OT (b), and P3BT (c) isothermally crystallized at an undercooling of 90 °C.

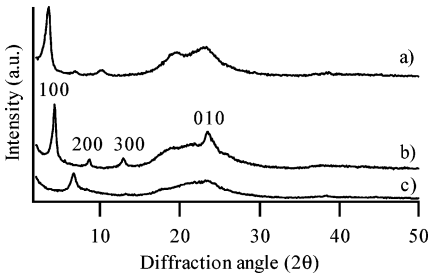

Figure 3. WAXS patterns of P3DDT (a), P3OT (b), and P3BT (c) isothermally crystallized at an undercooling of 75 °C. The indexing of the peaks is shown.

Table 2. Crystallization Temperature (T_c), Melting Temperature (T_m), and Melting Enthalpy (ΔH_m) of the Main Chains and Melting Temperature (T_{sc}) and Melting Enthalpy (ΔH_{sc}) of the Side Chains for P3BT, P3OT, and P3DDT Crystallized at the Three Different Undercoolings

ΔT (°C)	T_c (°C)	T_m (°C)	ΔH_m (J/g)	T_{sc} (°C)	ΔH_{sc} (J/g)
		P3BT			
60	262	243	15		
75	247	234	17		
90	232	222, 257	12		
		P3OT			
60	170	190	14		
75	155	188	15		
90	140	188	16		
		P3DDT			
60	118	155	16	64	3
75	103	157	13	63	2
90	88	156	15	63	2

n coefficients assume rather low values, which can be attributed to the rigid amorphous phase that acts as a hindrance for crystal growth since it does not promptly diffuse out from the crystal surface.[27,28] The n values are larger for P3BT than for P3OT and P3DDT because in the former the temperatures at which the measures were taken are much higher (and the undercooling correspondingly lower) with respect to P3OT and P3DDT, and thus, the process of diffusion of the amorphous fraction outward from the crystal surface can be a little more efficient.

Once T_m^0 had been determined, it was possible to prepare P3AT samples isothermally crystallized with a known undercooling. Three ΔT were chosen: 90, 75, and 60 °C (Table 2). It is very important when studying the crystallization behavior of different polymers to do so at the same undercooling because it is just this parameter that ensures that the systems being compared experienced the same thermal history.

The WAXS patterns of the samples thus prepared are shown in Figures 2−4.

The strong signal at smaller angles is indexed (100) (Figure 3) and associated to the side-by-side arrangement of the main chains.[1,4] Second- and third-order reflections, (200) and (300), are visible only in P3OT and P3DDT. These signals are associated with a higher degree of space filling and with a more significant interdigitation of the alkyl side chains.[1,29−31] The butyl side chains in P3BT, due to their short length and flexibility, do not efficiently intercalate, as opposed to longer alkyl lateral chains that can interact more effectively. When the number of carbon atoms in the side chains is more than 10, even side chain crystallization becomes possible.[2,12]

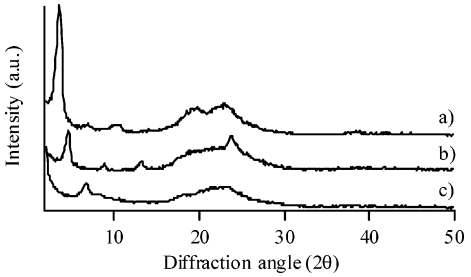

Figure 4. WAXS patterns of P3DDT (a), P3OT (b), and P3BT (c) isothermally crystallized at an undercooling of 60 °C.

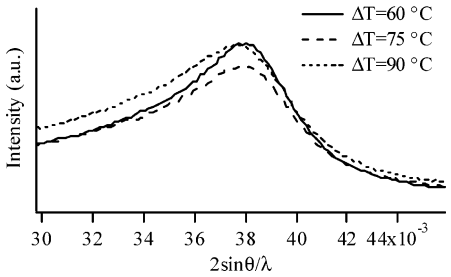

Figure 5. SAXS patterns of the (100) peak of P3DDT isothermally crystallized at different undercoolings.

It is quite obvious and well known[1−4,30] that the longer the side chain spacers, the further apart the neighboring coplanar main chains will be. What has not been thus far investigated is the effect of undercooling on the spacing of the main chains. It appears from our data that the structure of P3ATs, as observed by X-ray diffraction, is not influenced by the temperature of isothermal crystallization. The position of all the reflections does not in fact change. To obtain more accurate measurements of the d spacing of neighboring chains, SAXS has been employed. Figure 5 shows the results obtained for P3DDT: no shift in the (100) peak has been observed as a function of undercooling.

Analogous results were obtained for P3OT, while the (100) reflection of P3BT was at too wide angles to be detected by SAXS. On the basis of WAXS measurements, the same conclusions can be drawn for P3BT as well, since the (100) peak always appears at the same d spacing, irrespective of undercooling. The measured d_{100} distances were 13.1, 20.1, and 26.2 Å for P3BT, P3OT, and P3DDT, respectively. These values can be compared with those expected for a model in which the side chains are fully extended, namely, 13.1, 21.7, and 30.4 Å for P3BT, P3OT, and P3DDT, respectively.[1] It can be seen that while for P3BT there is excellent agreement, the measured data for P3OT and P3DDT are significantly lower. This is consistent with a model where partial intercalation occurs,[4] as evidenced[1,29−31] by the presence of (200) and (300) peaks in P3OT and P3DDT in which lateral chains interact more effectively than in P3BT, where such reflections are absent.

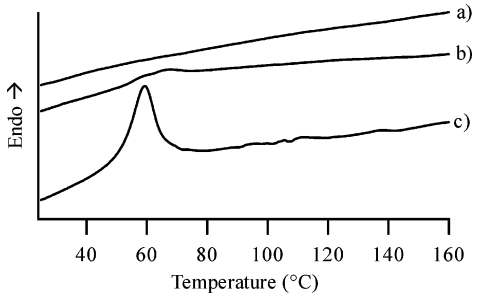

Figure 6. DSC heating traces, in the range 50−160 °C of P3BT crystallized at undercoolings of 90 (a), 75 (b), and 60 °C (c). Heating rate 10 °C/min. Nitrogen atmosphere.

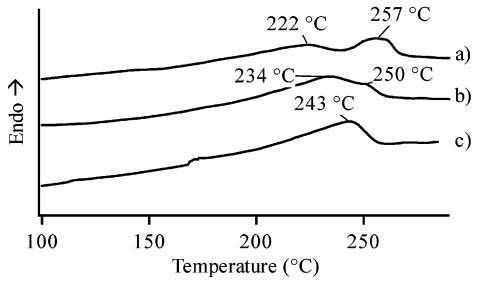

Figure 7. DSC heating traces, in the range 100−285 °C of P3BT crystallized at undercoolings of 90 (a), 75 (b), and 60 °C (c). Heating rate 10 °C/min. Nitrogen atmosphere.

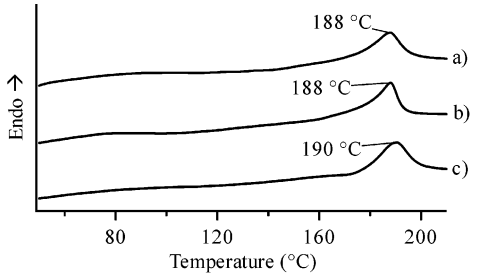

Figure 8. DSC heating traces of P3OT crystallized at undercoolings of 90 (a), 75 (b), and 60 °C (c). Heating rate 10 °C/min. Nitrogen atmosphere.

Another feature in the WAXS patterns of Figures 2−4 is a signal around 23−24° 2θ, indexed as (010) and associated with the stacking of the layers, formed by the chains arranged side-by-side. As can be seen, no substantial difference in the position of this reflection is observed. The distance between adjacent stacks is always the same, 3.8 Å, irrespective of the polymer and the undercooling. The broadness of this peak, which is superimposed to the amorphous halo centered around 20° 2θ, changes quite drastically in different polymers. While P3OT shows a distinct and neat peak, P3DDT and P3BT exhibit a much less defined (010) signal. This could be due to the presence of Phase II, as discussed further later in this paper.

The effect of undercooling was also investigated by DSC. Figures 6−9 show the heating traces of the samples crystallized at ΔT = 60, 75, and 90 °C. The thermograms of P3BT were divided in two ranges to enhance the peaks visible at lower (Figure 6) and higher temperatures (Figure 7).

As can be seen, apart from the expected shift of the melting temperatures toward higher values going from P3DDT to P3BT, the three samples exhibit markedly different behaviors. In Table 2 the thermal data obtained by such thermograms are shown. P3OT is the polymer with the most simple pattern (Figure 8).

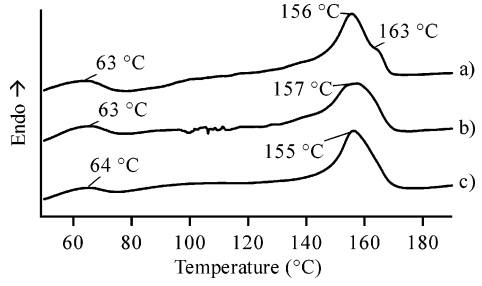

Figure 9. DSC heating traces of P3DDT crystallized at undercoolings of 90 (a), 75 (b), and 60 °C (c). Heating rate 10 °C/min. Nitrogen atmosphere.

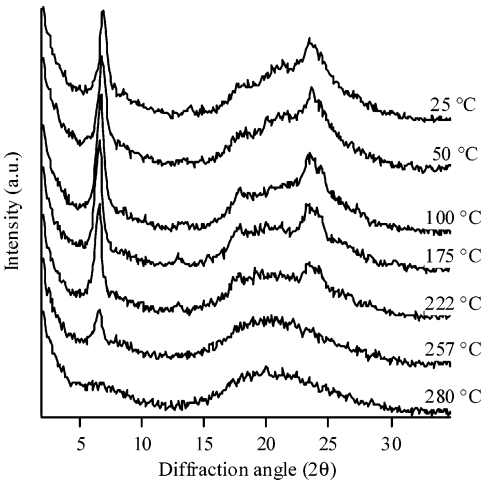

Figure 10. WAXS patterns of the P3BT sample crystallized at ΔT = 90 °C taken at 25, 50, 100, 175, 222, 257, and 280 °C.

Lowering the undercooling, the melting temperature slightly increases as expected but the endotherm is always a single and neat signal. The melting enthalpy is within the precision of the measurements (±1 J/g) constant, confirming that the undercooling does not induce, in this polymer, very important structural changes.

A different melting behavior characterizes both P3BT and P3DDT. It can be seen how, increasing the undercooling, the shape of the melting endotherm changes drastically, giving rise to a well developed double peak in P3BT (Figure 7) and an evident shoulder in P3DDT (Figure 9). Moreover, in P3DDT an endotherm is evident at about 63 °C at all the undercoolings (Figure 9), while in P3BT a peak appears between 50 and 100 °C in the samples isothermally crystallized at ΔT = 75 and 60 °C (Figure 6).

To clarify the nature of such DSC signals, temperature-controlled WAXS experiments were performed.

In Figure 10 the results pertaining to P3BT crystallized at ΔT = 90 °C are shown.

As can be seen, no appreciable change in the structure of the polymer is detectable until 257 °C, in correspondence with the second endotherm of Figure 7. At this temperature nearly all the material is already melted and just a residual order due to side-by-side arrangement is present. Beyond the second melting peak the stacking has completely disappeared. An analogous behavior was observed also by Bolognesi and co-workers[18] in low molecular weight P3OT and is consistent with the formation of two phases: Phase I and a mesophase, probably nematic in nature, that appears when some degree of twisting between adjacent thiophene units has taken place.[4,17,18,20,21] The me-

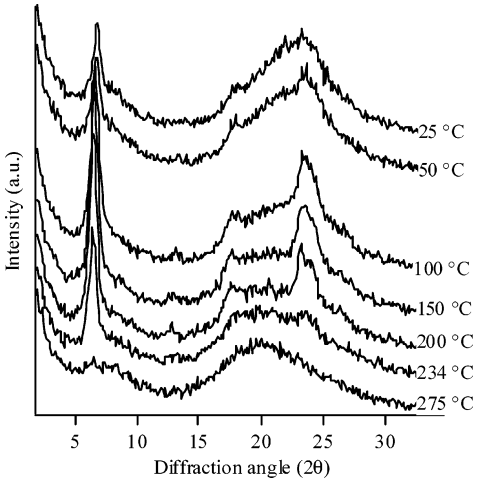

Figure 11. WAXS patterns of the P3BT sample crystallized at $\Delta T = 75$ °C taken at 25, 50, 100, 150, 200, 234, and 275 °C.

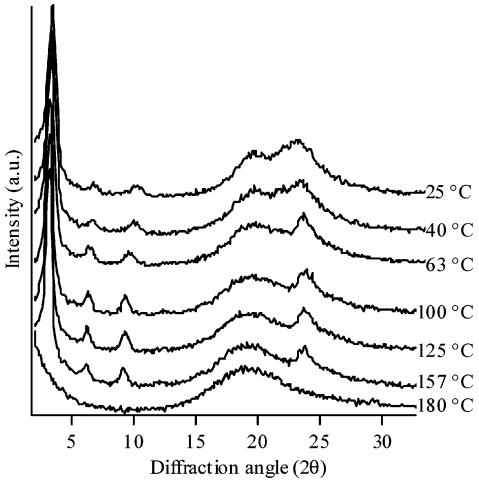

Figure 12. WAXS patterns of the P3DDT sample crystallized at $\Delta T = 75$ °C taken at 25, 40, 63, 100, 125, 157, and 180 °C.

sophase has an order due to side-by-side alignment but not to stacking because the twisting of thiophenes prevents the layers from efficiently and orderly interacting. The first melting peak in Figure 7 is thus related to the Phase I → mesophase transition, while the second corresponds to the isotropization of the polymer.

Although for the sample crystallized at $\Delta T = 75$ °C the heating trace shows just a broad-shouldered peak, different from P3BT with an undercooling of 90 °C that gives a well-developed double peak, temperature-controlled WAXS experiments show that the former sample passes through a nematic mesophase (Figure 11). It is notable, in fact, that the (010) peak has almost disappeared at 234 °C, in correspondence with the maximum of the peak that is ascribable to the Phase I → mesophase transition. Moreover, Figures 10 and 11 show a distinct double amorphous halo in the diffractograms taken after the isotropization temperature. It has been argued[11,32] that a maximum at a small angle like that observed is due to formation of a nematic mesophase.

Temperature-controlled WAXS measurements were performed on the P3BT samples crystallized at $\Delta T =$ 75 and 60 °C also to shed some light on the nature of the endotherms observable in the thermograms in Figure 6.

As can be seen in Figure 11, between 50 and 100 °C dramatic changes in the WAXS pattern are observed (the behavior of the sample crystallized at $\Delta T = 60$ °C was perfectly analogous). The (100) reflection becomes sharper and more intense, while the broad shoulder at around 7° 2θ disappears. At wider angles the (010) signal ($d_{010} = 3.8$ Å) emerges from the very broad halo in the 20−25° 2θ range. The amorphous halo maximum shifts to smaller angles, to 20° 2θ. Beyond the temperature of 100 °C, the WAXS pattern has the usual aspect expected for normal Phase I P3BT. The presence of Phase II was reported earlier for P3OT, P3DDT, and poly(3-decylthiophene).[13−16] The features characterizing this polymorph[14] are a series of low-angle signals very similar to (100), (200), and (300) of Phase I but shifted to wider angles. Moreover, a reflection due to interlayer stacking appears at about 20° 2θ, implying a stacking distance of 4.47 Å. Finally, the amorphous halo is shifted to a higher angle: 22.5° 2θ rather than about 20° 2θ, typical of Phase I. Phase II structure can be described as a system of stacked layers of interdigitated P3ATs, arranged side-by-side.[14] In the WAXS spectrum at room temperature, all Phase II signals are superimposed to those of Phase I, but beyond 100 °C Phase II reflections disappear, as described above. The endotherms in Figure 6 are then associated to a Phase II → Phase I transition. Thus far, Phase II was never detected in P3BT but just in P3ATs substituted with longer alkyl side chains. Furthermore, until now Phase II had been obtained only by crystallization from solution,[13−16] except in the case of low molecular weight systems.

A similar behavior was exhibited by P3DDT, crystallized at $\Delta T = 75$ °C (Figure 12).

The presence of Phase II is detectable in this sample as well. The sharpening of the (010) peak around 63 °C is evident as well as the shift of the amorphous halo toward smaller angles. Moreover, beyond the temperature of 63 °C, in correspondence with the maximum of the endotherm in Figure 9, the (200) and (300) reflections are much neater and shifted to smaller angles. These changes are consistent with a Phase II → Phase I transition.[14,15] In that region of the DSC trace there is also the melting signal of the crystallized side chains, which is known to occur in the 40−80 °C range in P3DDT.[2,19,20,30]

A temperature-dependent WAXS study of P3DDT samples was interesting to clarify the nature of the broadening and splitting into a double peak of the melting endotherm of the P3DDT crystallized at undercoolings of 90 and 75 °C. No change whatsoever was detected in the WAXS pattern taken at 156 and 163 °C on P3DDT crystallized at $\Delta T = 90$ °C (not shown). The double peak in Figure 9 is ascribable, as in the case of P3BT, to the presence of a Phase I → nematic mesophase transition and to the complete isotropization of the sample, respectively.[4,17,20,21] Different from P3BT, though, these two phases are not distinguishable from a crystallographic point of view in P3DDT.[20] This is probably due to the long and flexible dodecyl side chains that preserve a similar framework of the chains.

Last, temperature-controlled WAXS was applied to P3OT crystallized at $\Delta T = 75$ °C. As can be seen in Figure 13, no appreciable changes in the appearance of the diffraction patterns are visible.

The reflections associated with the side-by-side arrangement and stacking of the layers remain visible until complete melting, which happens at 225 °C. The only effect experienced by the sample during heating is

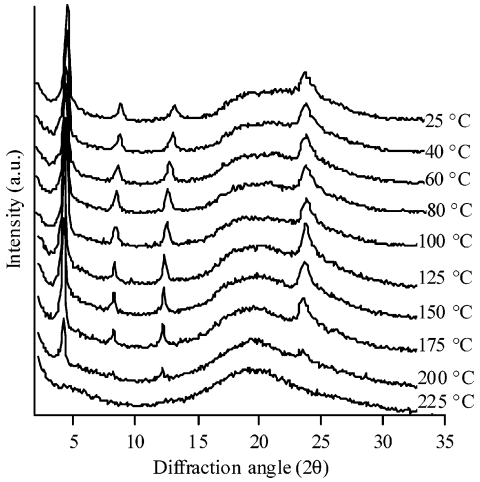

Figure 13. WAXS patterns of the P3OT sample crystallized at $\Delta T = 75$ °C taken at 25, 40, 60, 80, 100, 125, 150, 175, 200, and 225 °C.

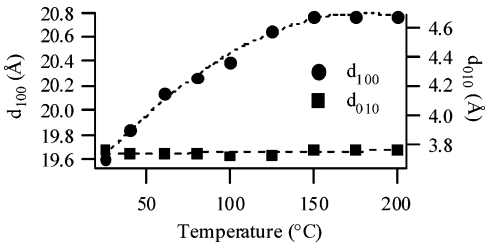

Figure 14. *d*-Spacing of the (100) (left axis) and (010) (right axis) reflections of the P3OT sample crystallized at $\Delta T = 75$ °C as a function of temperature.

a shift toward lower angles of the (100), (200), and (300) peaks. Figure 14 shows the change in the *d* spacing of (100) and (010) peaks as a function of temperature.

This is a well-known phenomenon.[4,17,33,34] At low temperatures, the main chain and the alkyl side chains are in an almost extended trans conformation. As the temperature rises, a conformational change from trans to gauche is initiated and the thermal agitation of the alkyl side chains triggers a twisting of the thiophene rings as well. This brings about the changes in the *d* spacing observed in Figure 14[13,17] and is at the basis of the thermochromic behavior of P3ATs. No polymorphism was detected in this case. As proposed by Bolognesi and co-workers,[18] many factors contribute to the polymorphism tendency in P3ATs, the low molecular weight being the most important of them.[15,18] At a molecular level, the prevalent property in determining polymorphism is the ratio between the length of the chains and their lateral hindrance with in-chain defects and side chain length as relevant factors too. Both P3OT and P3DDT had a rather high polymerization degree, but the reduced lateral hindrance due to the shorter octyl moieties probably determined the appearance of multiple phases in P3DDT.

Conclusion

In the course of this study, the following findings have been made.

T_m^0 of P3BT, P3OT, and P3DDT are 321, 230, and 175 °C, respectively: the shorter the alkyl side chains, the less flexible is the polymer.

Crystallization proceeds by heterogeneous nucleation, with one-dimensional linear growth. The small Avrami *n* coefficients measured imply that the rigid amorphous fraction has a key role in hindering the crystallization mechanism.

When increasing the side chain length, the spacing of the coplanar P3AT chains increases because the alkyl side chains act as spacers between them. Interdigitated structures are less numerous in P3BT due to the poor flexibility of the butyl moieties, while in the case of P3OT and P3DDT they coexist with end-to-end arrangements.

In conclusion, some remarks can be made regarding each of the polymers studied.

P3BT. This polymer has the highest T_m^0 of those studied, its macromolecular chains being the least flexible. The short butyl side chains are not mobile and adaptable like those of P3OT and P3DDT, so they determine a slower crystallization rate and the scarce interdigitation in the side-by-side arrangement of the main chains in Phase I. Two very interesting features were noted for this polymer.

As the undercooling increases, a double peak in the DSC melting pattern appears. This is due to the presence of a Phase I → nematic mesophase transition, followed by isotropization of the polymer. The mesophase is characterized by the absence of order due to stacking. This is mainly due to the shortness of the butyl side chains that cannot preserve the stacking of the layers when twisting of the thiophene rings occur.

The presence of polymorphism was also detected. Phase II coexisted with Phase I in P3BT crystallized at $\Delta T = 75$ and 60 °C, but it transformed into Phase I between 50 and 100 °C. This transition appeared in the DSC trace as well.

P3BT, when crystallized from the melt, gives rise mainly to an ordinate Phase I structure that transforms into a nematic mesophase when it is heated. When particular conditions of undercooling are met, namely, in this work $\Delta T = 75$ and 60 °C, Phase II also appears.

P3OT. P3OT does not show any double peak in its DSC melting thermogram, and no evidence of polymorphism was found. It seems that the intermediate side chain length of octyl moieties is the optimum for the formation of a pure ordinate Phase I structure. Disorder can be induced in the crystalline framework by raising the temperature, with the effect of twisting and tilting adjacent thiophene rings, pursuing a semi-ordinate arrangement.

P3DDT. This polymer also exhibits polymorphism. The transition Phase II → Phase I takes place at about 60 °C and can be detected by an evident endotherm in the DSC trace. Phase I then is transformed into a nematic mesophase. Different from P3BT, though, these two phases cannot be differentiated by X-ray diffraction. The long dodecyl chains can, with their flexibility, counteract the disordering effect of the twisting of polythiophene chains and, by the means of positive interactions, preserve the reflections associated with the stacking of the layers.

Acknowledgment. The financial support of the Ministero dell'Università e della Ricerca Scientifica e Tecnologica (MURST) of Italy, by means of the PRIN project "New hybrid functional materials based on carbon nanotubes-polymer matrix for photovoltaic devices", is gratefully acknowledged. The authors of the present work are part of the Consorzio Interuniversitario Nazionale di Scienza e Tecnologia dei Materiali (INSTM) network.

References and Notes

(1) Chen, S.-A.; Ni, J.-M. *Macromolecules* **1992**, *25*, 6081.
(2) Hsu, W.-P.; Levon, K.; Ho, K.-S.; Myerson, A. S.; Kwei, T. K. *Macromolecules* **1993**, *26*, 1318.
(3) Chen, T.-A.; Wu, X.; Rieke, R. D. *J. Am. Chem. Soc.* **1995**, *117*, 233.
(4) Yang, C.; Orfino, F. P.; Holdcroft, S. *Macromolecules* **1996**, *29*, 6510.
(5) McCullough, R. D. *Adv. Mater.* **1998**, *10*, 93.
(6) Prosa, T. J.; Winokur, M. J.; Moulton, J.; Smith, P.; Heeger, A. J. *Macromolecules* **1992**, *25*, 4364.
(7) Corish, J.; Morton-Blake, D. A.; Bénière, F.; Lantoine, M. *J. Chem. Soc., Faraday Trans.* **1996**, *92*, 671.
(8) Tashiro, K.; Kobayashi, M.; Kawai, T.; Yoshino, K. *Polymer* **1997**, *38*, 2867.
(9) Xie, H.; Corish, J.; Morton-Blake, D. A.; Aasmundveit, K. E. *Synth. Met.* **2000**, *113*, 65.
(10) Yamamoto, T.; Komarudin, D.; Arai, M.; Lee, B.-L.; Suganuma, H.; Asakawa, N.; Inoue, Y., Kubota, K.; Sasaki, S.; Fukuda, T.; Matsuda, H. *J. Am. Chem. Soc.* **1998**, *120*, 2053.
(11) Winokur, M. J.; Spiegel, D.; Kim, Y.; Hotta, S.; Heeger, A. J. *Synth. Met*. **1989**, *28*, C419.
(12) Ho, K.-S.; Bartus, J.; Levon, K.; Mao, J., Zheng, W.-Y. *Synth. Met.* **1993**, *55*−*57*, 384.
(13) Bolognesi, A.; Porzio, W.; Provasoli, F.; Ezquerra, T. *Makromol. Chem.* **1993**, *194*, 817.
(14) Prosa, T. J.; Winokur, M. J.; McCullough, R. D. *Macromolecules* **1996**, *29*, 3654.
(15) Meille, S. V.; Romita, V.; Caronna, T.; Lovinger, A. J.; Catellani, M.; Belobrzeckaja, L. *Macromolecules* **1997**, *30*, 7898.
(16) Bolognesi, A.; Porzio, W.; Provasoli, A.; Botta, C.; Comotti, A.; Sozzani, P.; Simonutti, R. *Macromol. Chem. Phys.* **2001**, *202*, 2586.
(17) Tashiro, K.; Ono, K.; Minagawa, Y.; Kobayashi, M.; Kawai, T.; Yoshino, K. *J. Polym. Sci., Polym. Phys. Ed.* **1991**, *29*, 1223.
(18) Bolognesi, A.; Porzio, W.; Zhuo, G.; Ezquerra, T. *Eur. Polym. J.* **1996**, *32,* 1097.
(19) Malik, S.; Nandi, A. K. *J. Polym. Sci., Polym. Phys. Ed.* **2002**, *40*, 2073.
(20) Park, K. C.; Levon, K. *Macromolecules* **1997**, *30*, 3175.
(21) Liu, S. L.; Chung, T. S. *Polymer* **2000**, *41*, 2781.
(22) Hoffman, J. D.; Weeks, J. J. *J. Res. Natl. Bur. Stand. U.S.A.* **1962**, *A66,* 13.
(23) Avrami, M. *J. Chem. Phys.* **1939**, *7*, 1103.
(24) Avrami, M. *J. Chem. Phys.* **1940**, *8*, 212.
(25) Avrami, M. *J. Chem. Phys.* **1941**, *9*, 177.
(26) Clark, E. J.; Hoffman, J. D. *Macromolecules* **1984**, *17*, 878.
(27) Cheng, S. Z. D.; Wunderlich, B. *Macromolecules* **1988**, *21*, 3327.
(28) Cheng, S. Z. D. *Macromolecules* **1988**, *21*, 2475.
(29) Chen, S.-A.; Lee, S.-J. *Polymer* **1995**, *36*, 1719.
(30) Qiao, X.; Wang, X.; Mo, Z. *Synth. Met.* **2001**, *118*, 89.
(31) Qiao, X.; Xiao, X.; Wang, X.; Yang, J.; Qiu, Z.; An, L.; Wang, W.; Mo, Z. *Eur. Polym. J.* **2002**, *38*, 1183.
(32) Winokur, M. J.; Wamsley, P.; Moulton, J.; Smith, P.; Heeger, A. J. *Macromolecules* **1991**, *24*, 3812.
(33) Tashiro, K.; Ono, K.; Minagawa, Y.; Kobayashi, M.; Kawai, T.; Yoshino, K. *Synth. Met.* **1991**, *41*−*43*, 571.
(34) Chen, S.-A.; Lee, S.-J. *Synth. Met.* **1995**, *72*, 253.

MA048159+